SUPPORTING INFORMATION

Oxidation of *sp*- and sp^2-hybridised Molecular Semiconductors with Iron(III) Chloride in Organic Media

Elda Sala,[1,2] João Paulo V. Damasceno,[3,*] Stefano Pecorario,[4] Pietro Marabotti,[5] Ivan K. Ilic,[1] Valerio Galli,[1,6] Simone Melesi,[2] Pierfrancesco Sansò,[1,2] Andrea Tuarivoli,[1,2] Carlo S. Casari,[2] Daniele Fazzi,[7] Rik R. Tykwinski,[8] Mario Caironi[1,*]

[1]Center for Nano Science and Technology, Istituto Italiano di Tecnologia (IIT), Milano (20134), Italy; [2]Department of Energy, Micro and Nanostructured Materials Laboratory - NanoLab, Politecnico di Milano, Milano (20133), Italy; [3]Department of Inorganic Chemistry, Institute of Chemistry (IQ), University of Campinas (UNICAMP), Campinas (13083-970), Brazil; [4]Cavendish Laboratory, University of Cambridge, Cambridge, UK; [5]Institut für Physik, Humboldt Universität zu Berlin, Berlin (12489), Germany; [6]Department of Physics, Politecnico di Milano, Milano (20133), Italy; [7]Department of Chemistry "Giacomo Ciamician", University of Bologna, Bologna (40129); [8]Department of Chemistry, University of Alberta, Edmonton, Canada.

Corresponding Authors:

JPVD: joaopvd@unicamp.br

MC: mario.caironi@iit.it

Experimental procedure

Materials

Anhydrous $FeCl_3$ (≥99.99 %; MM = 162.2 g mol^{-1}), chloroform (CF, anhydrous, ≥99 %, with 0.5-1.0 % of ethanol as a stabiliser), acetonitrile (ACN, anhydrous, 99.8 %), tetrahydrofuran (THF, anhydrous, ≥99.9 %), nitromethane (NM, absolute, ≥98.5 %), tetrabutylammonium tetrafluoroborate (99 %; referred as [(TBA)(TFB)]), dichloromethane (≥99.8 %, with amylene as stabiliser), and ferrocene (98 %) were acquired from Sigma-Aldrich. The described solvents were acquired in sealed bottles and collected inside a glove box using glass syringes and stainless steel needles. Tetraphenyl butatriene, also known as tetraphenyl[3]cumulene (henceforth referred to as [3]Ph; MM = 356.446 g mol^{-1}), was synthesised according to the procedures reported elsewhere and reviewed by Wendinger and Tykwinski.[1] 2,7-Dioctyl[1]benzothieno[3,2-b][1]benzothiophene (C8-BTBT) was acquired from Sigma-Aldrich. Typical O_2 and H_2O concentrations during experiments in the glovebox (Siemens, MB 200B) are ~0.4 and ≤0.1 ppm, respectively. Crystal structures of $FeCl_3$ were rendered using the free software VESTA (version for Linux), and the structural parameters of this solid were collected from the Crystallography Open Database (COD ID 1535681).

Dissolution of $FeCl_3$ and mixtures with [3]Ph solutions

A solution of $FeCl_3$ 12 g L^{-1} was prepared in chloroform (1 mL) by stirring solid and solvent in a glass vial for 1 h and inside a glovebox. A solution of [3]Ph 3 g L^{-1} in chloroform (1 mL) was prepared following the same conditions. After the dilutions of $FeCl_3$, the solution of [3]Ph was added to reach a specific final concentration. Initially, concentrated $FeCl_3$ (12 g L^{-1}) was diluted with chloroform and a second solvent, the last being equal to half of the final volume (500 μL). Then, a portion of [3]Ph solution (3 g L^{-1}) was added. Typically, a mixture with 0.25 g L^{-1} [3]Ph and 0.75 g L^{-1} $FeCl_3$ (final concentrations) was prepared by adding 62.5 μL of 12 g L^{-1} $FeCl_3$ in a 1 mL quartz cuvette (with polymeric cap, solvent resistant), followed by 354.5 μL of chloroform, 500 μL of another solvent (ACN, NM, THF, or chloroform) and 83 μL of 3 g L^{-1} [3]Ph, respectively. All mixtures were prepared similarly, but adding more concentrated solutions, less chloroform, and the same volume of the second solvent. All experiments were performed keeping the final mass proportion of [3]Ph to $FeCl_3$ equal to 1:3 (equivalent to 1:6.6 in mol), while absolute concentrations were varied because oxidation-induced spectral features become evident only above a minimum concentration range, even at constant ratio. All analyses were performed with fresh solutions just after mixing. (Caution note: $FeCl_3$ is highly corrosive and demands precautions for manipulation[2]).

Dissolution of $FeCl_3$ and mixtures with C8-BTBT solution

The concentrated mixture of $FeCl_3$ in chloroform (12 g L^{-1}) was diluted with chloroform or another solvent (ACN, NM, THF, or chloroform) in a glovebox to achieve the desired final concentration. A solution of semiconductor C8-BTBT (5.21 g L^{-1}) in chloroform was prepared following the previous conditions. After the dilutions of $FeCl_3$ with chloroform and a second solvent, the C8-BTBT solution was added to reach a specific final concentration. Typically, the final concentrations of $FeCl_3$ and C8-BTBT were 5.4 and 0.13 g L^{-1}, respectively. All analyses were performed with fresh solutions just after mixing.

Diluted $FeCl_3$ in pure solvents or mixtures

A solution of $FeCl_3$ 3 g L^{-1} was prepared in chloroform following the previous procedure. Then, chloroform and/or other solvents were added to dilute the systems to different concentrations as indicated below. The final concentration of the solution was chosen depending on the analyses performed: 0.02 g L^{-1} for UV-Vis-NIR analyses, 0.75 g L^{-1} for homocoagulation experiments, and 0.01 or 0.1 g L^{-1} for DLS measurements. For Raman analyses, solutions of $FeCl_3$ 12.0 g L^{-1} were used.

Homocoagulation of $FeCl_3$ in solvents with tetrabutylammonium tetrafluoroborate solutions

Two sets of experiments were performed with different concentrations of $FeCl_3$ (1.5 or 0.1 g L^{-1}), both using the same concentrations of electrolyte. The mixtures were prepared by mixing 450 µL of $FeCl_3$ dispersion and 450 µL of the respective electrolyte solution in 2 mL glass vials, the second is 2 times more concentrated than the final concentration indicated and the final $FeCl_3$ concentrations are half of the initials (0.75 or 0.05 g L^{-1}). The mixtures have final electrolyte concentrations in both sets of experiments equal to 5×10^{-6}, 1×10^{-5}, 5×10^{-5}, 1×10^{-4}, 5×10^{-4}, 1×10^{-3}, 5×10^{-3} and 1×10^{-2} mol L^{-1} (already considering the dilution by a factor of 2 after mixing with $FeCl_3$ dispersion). Samples were homogenised and left to rest for 12 h. Then, pictures of the vials were taken.

Electrochemical measurements and Raman spectroelectrochemistry

The cyclic voltammetry was carried out with a MultiPalm Sens4 potentiostat using platinum wires as working and reference electrodes and a thick gold wire as counter-electrode, and ferrocene as internal reference. After a few optimisation experiments, the concentrations of supporting electrolyte [(TBA)(TFB)], ferrocene and [3]Ph were fixed as 0.1 mol L^{-1}, 1.0×10^{-3} mol L^{-1} and 0.1 g L^{-1}, respectively, using dichloromethane as solvent.

Raman spectroelectrochemistry analyses were performed focusing the green laser (532 nm) of a Renishaw InVia micro Raman spectrometer onto a platinum grid used as the working electrode. A platinum wire and a thick gold wire were used as reference and counter-electrode, respectively. The grating selected (1800 lines mm^{-1}) allowed a good resolution and spectral region (1550 to 3050 cm^{-1}), covering from the phenyl breathing mode to the CH stretching mode of the solvent. Raman spectra were acquired with a 20× objective, an acquisition time of 1 s and a laser power of 70 mW while keeping the potential between the working and the reference electrodes at +1.05 V, and using a 0.65 g L^{-1} [3]Ph solution in dichloromethane well protected from the ambient atmosphere.

Materials characterisation

UV-Vis-NIR spectra measurements were conducted in a Perkin Elmer spectrometer, model Lamba 1050, scanning from 200 (or 250) to 800 (or 1200) nm. The absorption blanks were collected in air and the measurements were performed using a quartz cuvette with a polymeric cap (4 or 10 mm of optical path). Raman spectra of $FeCl_3$ in the solid state, dissolved in chloroform or chloroform and acetonitrile mixture were acquired in a Renishaw spectrometer, model InVia Raman Microscope, using a red laser (785 nm), grating with 1200 lines mm^{-1} and calibration was performed with Si at 520.7 cm^{-1}. $FeCl_3$ samples were measured inside quartz tubes, filled with solid or liquid mixtures inside a glove box and kept closed. The spectra were acquired with an objective lens of 20×, using 10 to 15 s of integration time and 1 or 2 accumulations, and delivering 40 or 80 mW of laser power to the samples. Raman spectra of $FeCl_3$ mixed with [3]Ph solutions were acquired in a Renishaw inVia Raman microscope, equipped with a solid state laser (532 nm). The spectra acquisition was performed in a static mode, with grating of 1800 lines mm^{-1}, and an objective lens of 50×. Dynamic light scattering (DLS) was performed in Malvern equipment, model Zetasizer Nano series (Nano-ZS), using quartz cuvette at 23 °C and equilibrium time equal to 30 s before each analysis. The respective properties of each solvent or mixture were considered in each measurement. For each sample, five measurements were performed and four scans for each.

Quantum-chemical calculations.

Quantum-chemical calculations at the DFT level were carried out to assess the molecular, electronic, and vibrational structure of neutral and charged states. The range-separated exchange correlation functional wB97X-D functional was selected together with the cc-pVTZ basis set. The charged state (doublet spin multiplicity) was treated with the spin-polarised unrestricted approach (UwB97X-D). The molecular structure of both neutral and charged (+1) states was optimised and frequency calculation revealed stable minimum geometries. Raman spectra were computed for both neutral and charged states. Excited states (i.e., vertical transitions) were computed at the TD-DFT level by using

the same functional and basis set as for the geometry and frequency calculations. More than 20 excited states were computed for both neutral and charged states. Calculations were performed with Gaussian16/B01 version.

Additional Characterisation

Fig. S1 presents the UV-Vis absorption spectra of solutions of [3]Ph and $FeCl_3$ in chloroform (CF) at different concentrations. The full range is shown in **S1A**, while an expansion of the visible-near infrared range is displayed in **S1B**.

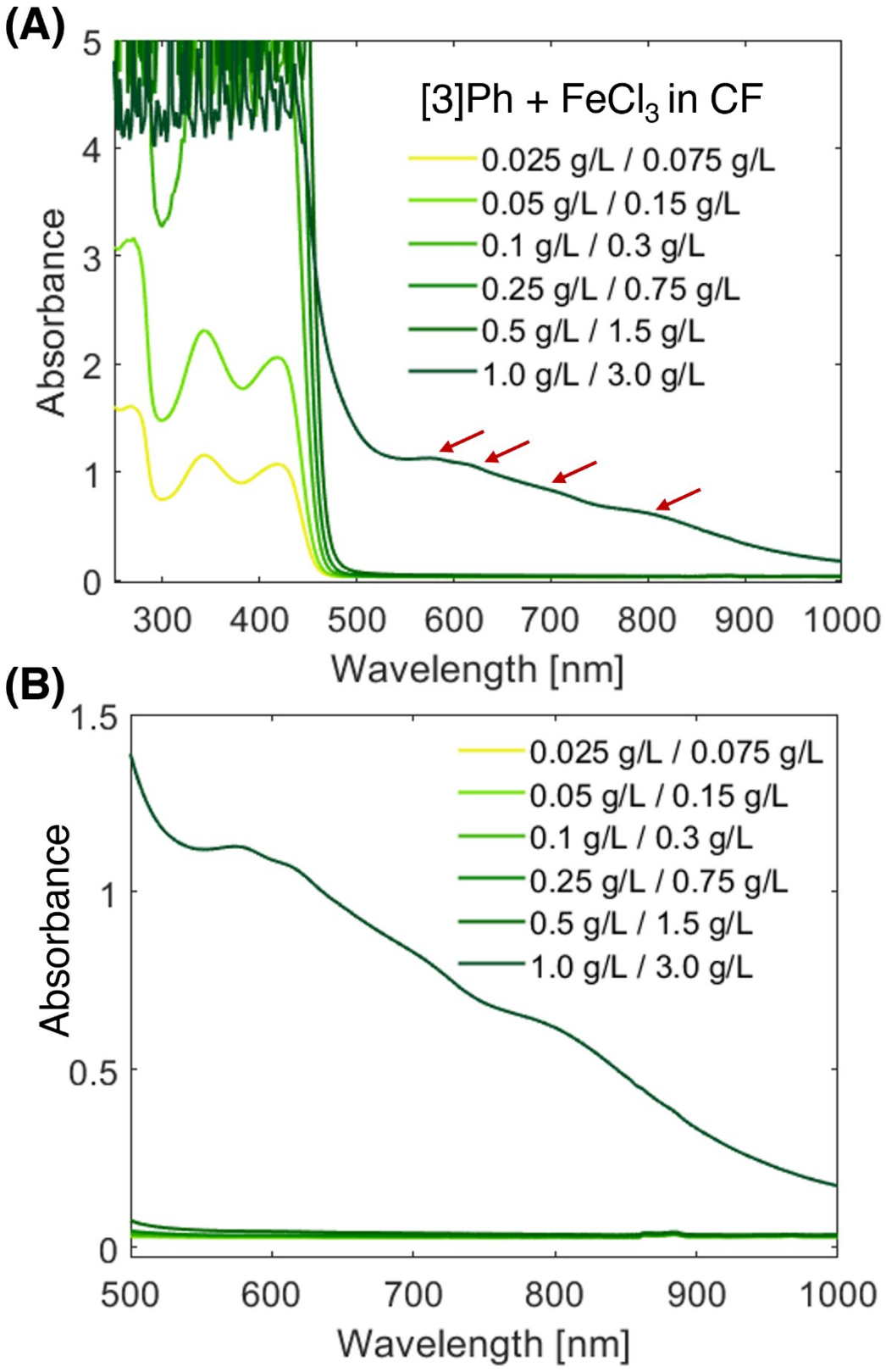

Fig. S2.1 shows TD-DFT vertical excitation energies for neutral and charged [3]Ph. On the right, the computed SOMOa and SUMOa for the [3]Ph^{+} are reported.

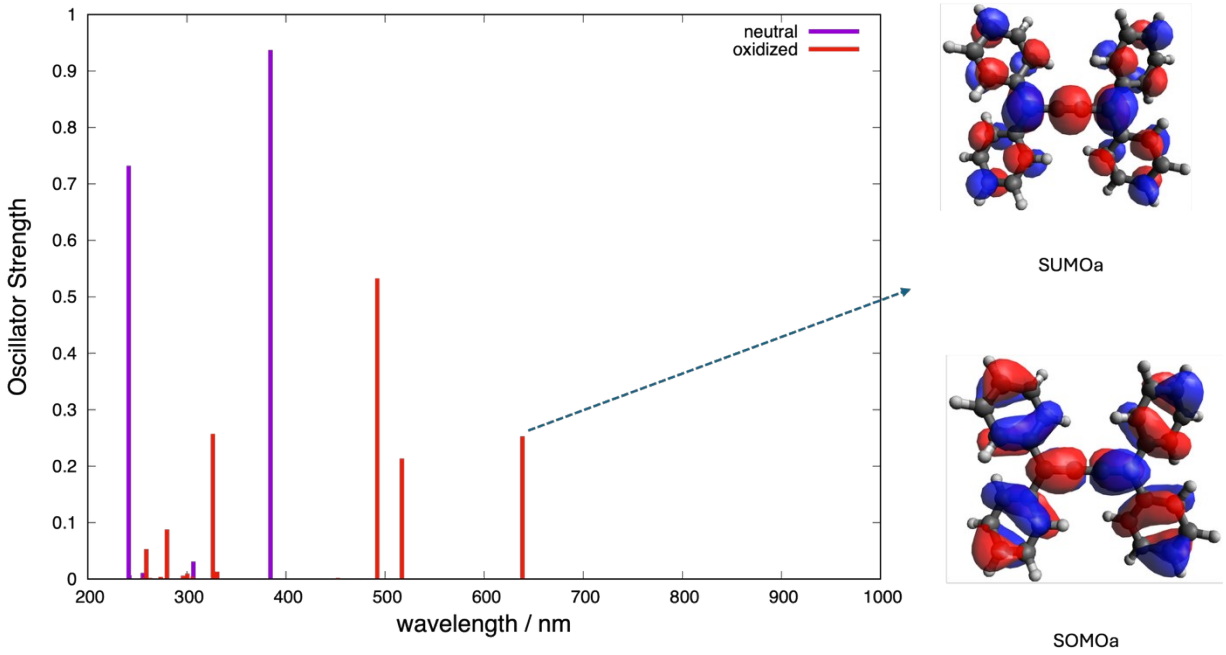

Fig. S2.2 shows DFT Raman spectra for neutral (violet) and charged (oxidised, red) species [3]Ph and [3]Ph^{+}. Unscaled frequencies.

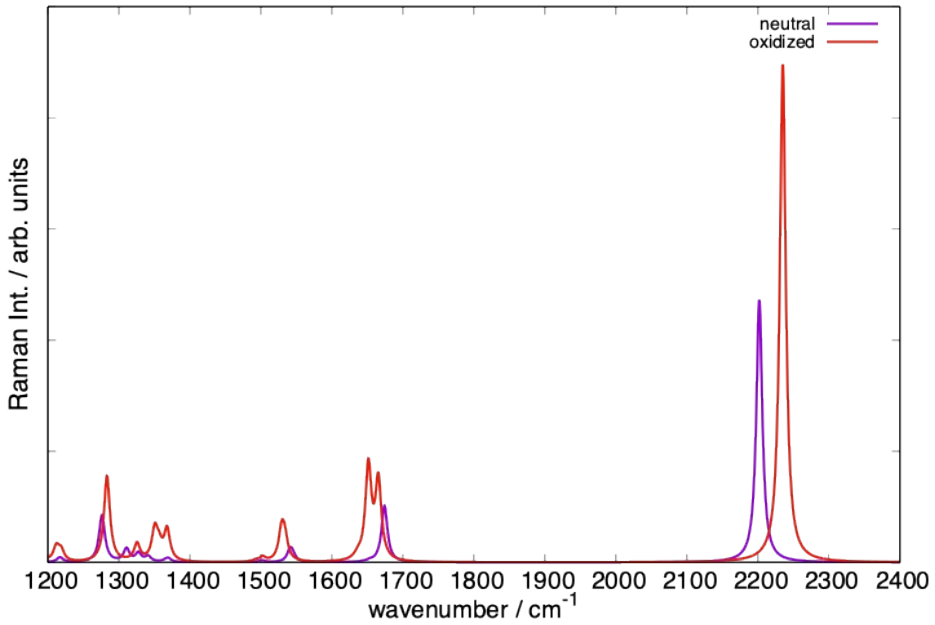

Fig. S3 shows DFT (ωB97X-D/cc-pVTZ) Bond Length Alternation along the sp-chain for neutral [3]Ph (green) and [3]Ph^+ (blue). 0 is the central carbon-carbon bond, -1 and +1 the nearest carbon bonds.

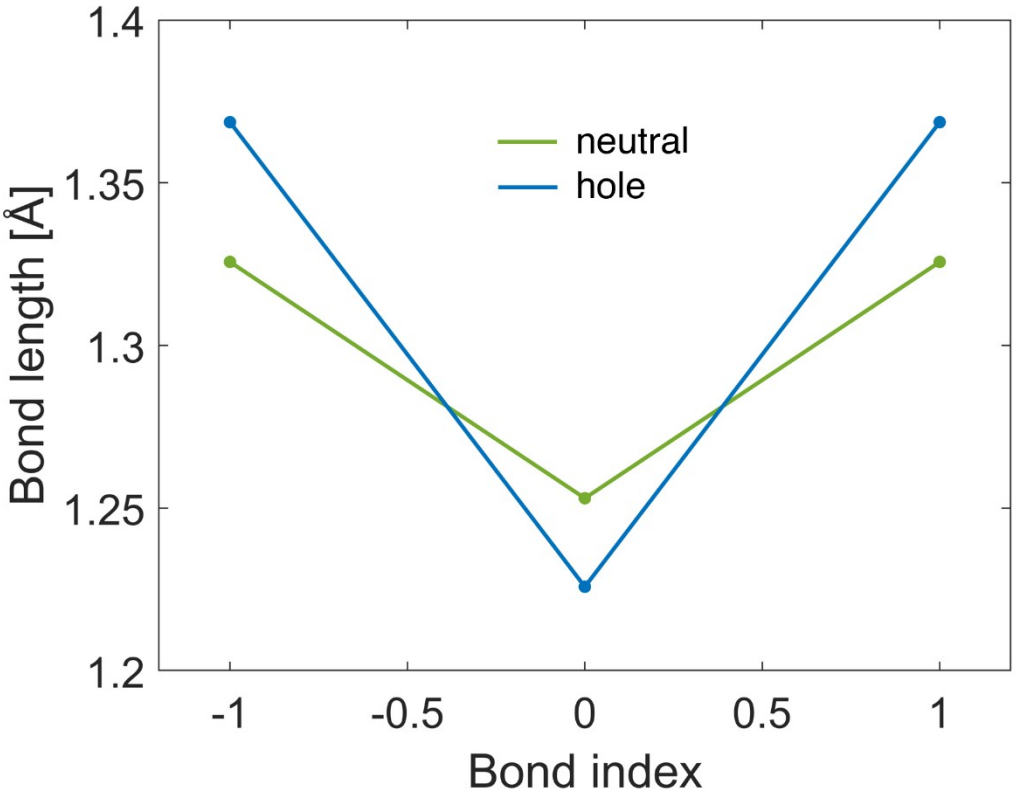

Fig. S4 presents the normalised Raman spectra of two $FeCl_3$ mixtures, the top one at a concentration of 4.5 g L^{-1} in CF-ACN (1:1 by volume), the bottom one at 0.75 g L^{-1} CF-NM (1:1 by volume). The signals shown in such spectra, i.e. the one at 2300 cm^{-2} for the CF-ACN spectrum and that at 1400 cm^{-2} in the CF-NM spectrum, are related to the solvents, ACN and NM respectively.[3,4]

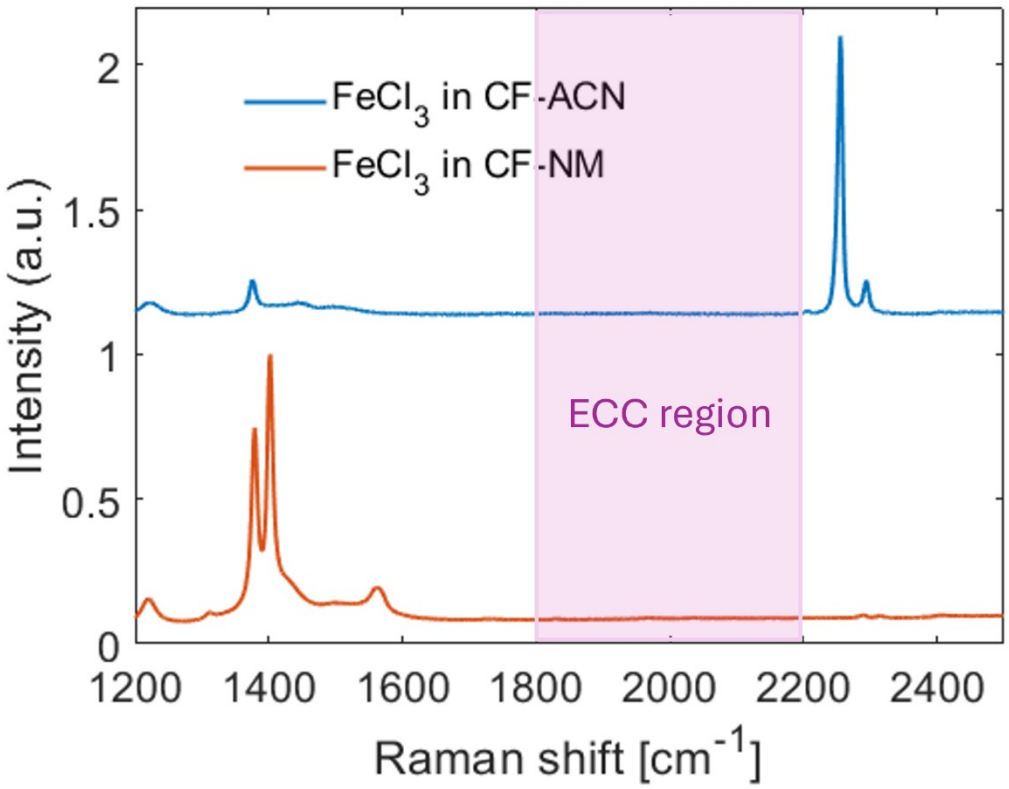

Fig. S5 presents the cyclic voltammograms of pure dichloromethane and ferrocene solution 1.0×10^{-3} mol L^{-1} in dichloromethane. Analyses were conducted with a rate of 50 mV s^{-1}, using [(TBA)(TFB)] 0.1 mol L^{-1} as a supporting electrolyte and under oxygen atmosphere. Such results demonstrate that the solvent is stable in this potential range and that there is no electrochemical signal at about +0.8 V in mixtures without [3]Ph.

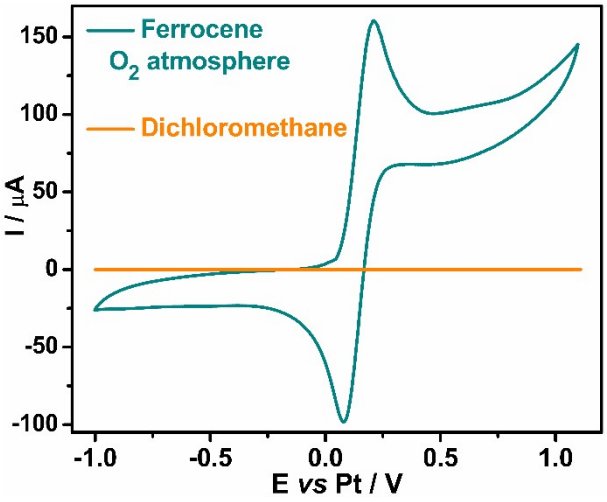

Fig. S6 presents the UV-Vis-NIR absorption spectra of C8-BTBT (0.13 g L^{-1}) mixed with $FeCl_3$ (5.4 g L^{-1}) in CF or solvent mixtures 1:1 by volume. The solvents added to CF are ACN, THF, and NM. In black, the spectrum of a diluted solution of pristine C8-BTBT (0.052 g L^{-1}) in CF. All spectra were acquired on 4 mm quartz cuvettes.

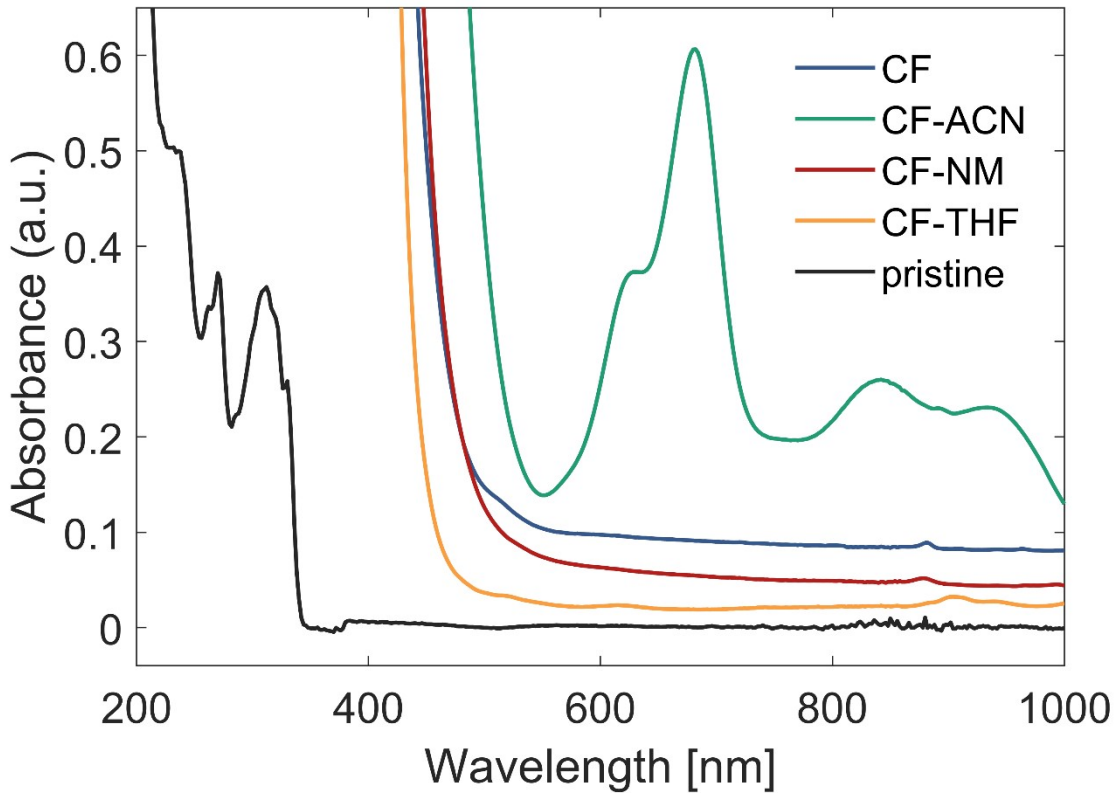

Fig. S7 reports pictures of $FeCl_3$ 0.75 g L^{-1} in chloroform or solvent mixtures (1:1, volume) irradiated by a green laser, from left to right, top to bottom: (a) chloroform (CF), and (b) CF-NM, (c) CF-ACN, and (d) CF-THF.

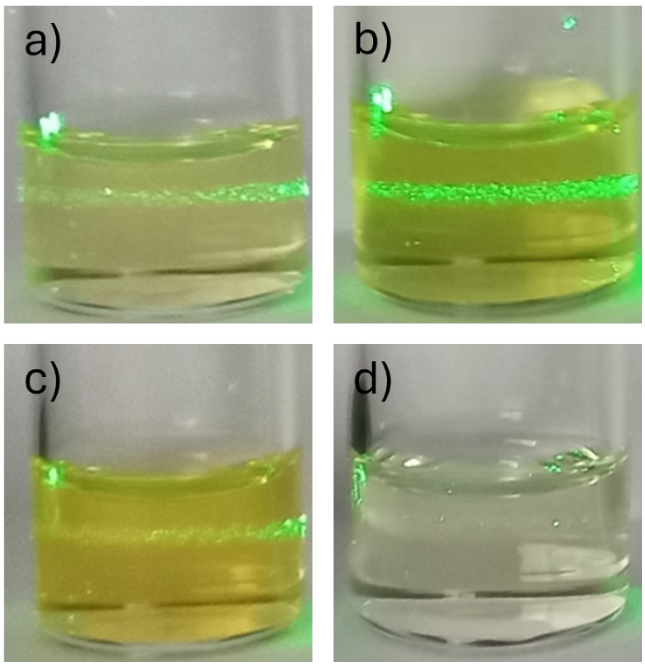

Fig. S8 presents the DLS results of two different concentrations of $FeCl_3$ in chloroform, ACN, NM, and THF. In **S8A**, DLS results of $FeCl_3$ (1 and 10 %) in tetrahydrofuran are shown. The letters (a) and (b) indicate two different batches and concentrations of 1 and 10 % mean 0.01 and 0.1 g L^{-1}, respectively. In **S8B**, dynamic light scattering (DLS) results from $FeCl_3$ in chloroform, ACN, or NM are presented. Concentrations of 1 and 10 % mean 0.01 and 0.1 g L^{-1}, respectively

In all mixtures, the diameters are bigger at higher concentrations of $FeCl_3$.

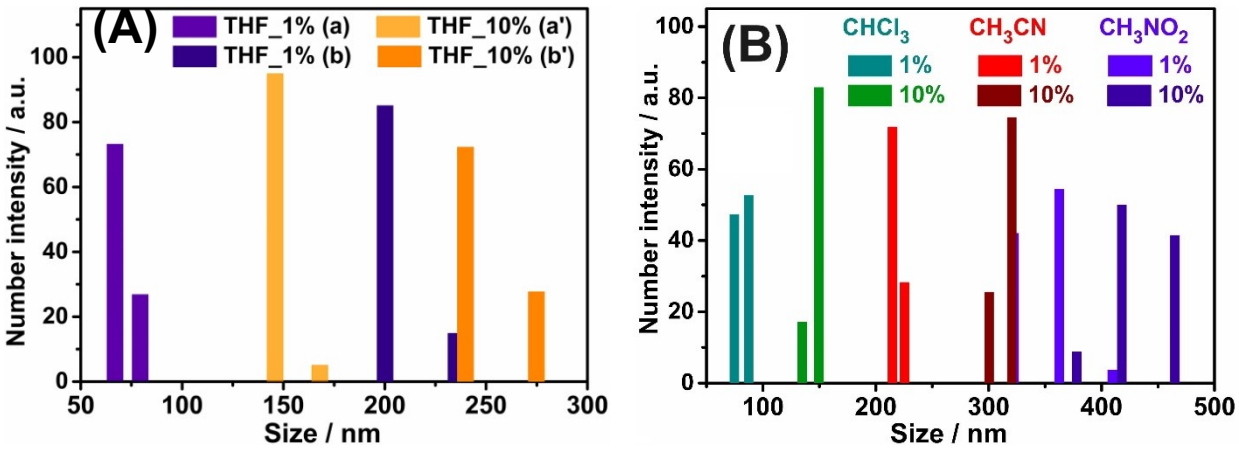

The DLS measurements for the THF-containing mixtures are noisier than the others and there is a higher signal variation for each sample, which indicates higher dissolution of the solid $FeCl_3$.

Fig. S9. (A) UV-Vis spectra of $FeCl_3$ 0.02 g L^{-1} in pure solvents or liquid mixtures (1:1, volume) according to the internal labels (10 mm cuvette). (B) Raman spectra of $FeCl_3$ in solid state or dissolved (12 g L^{-1}) in CF, ACN or CF-ACN (mixture 1:1, volume), along with spectra of pure solvents.

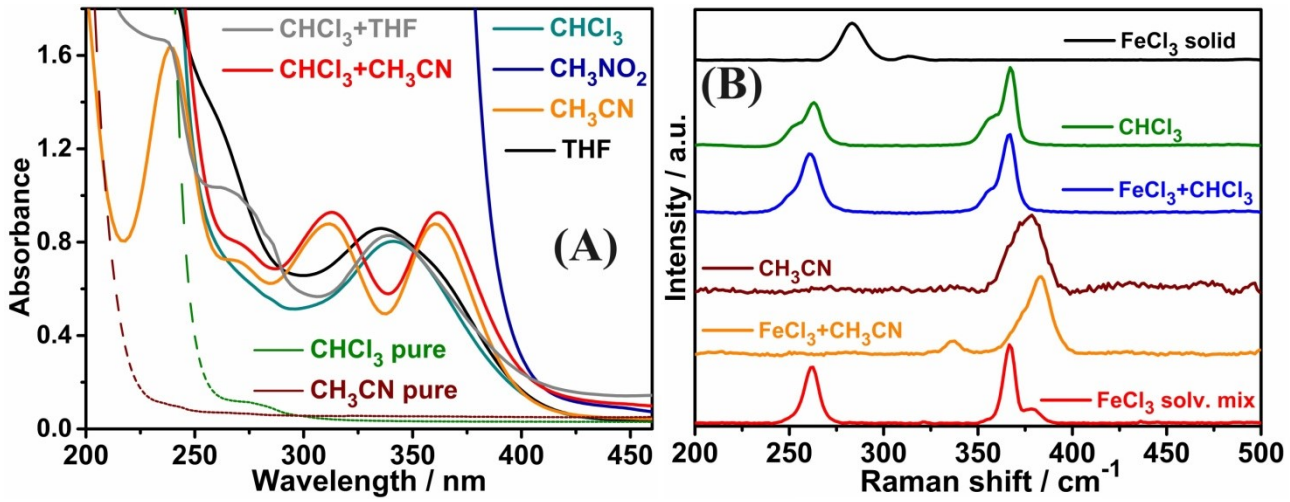

$FeCl_3$ in chloroform presents a band at 341 nm as mentioned before. However, this band is broad and can hide possible contributions around the maximum, although none is well-defined. In THF, $FeCl_3$ presents a similar absorption profile as in chloroform, but with higher absorbance, indicating a higher concentration of soluble monomeric $FeCl_3$.[5,6] The absorbance maximum is slightly blue-shifted at 335 nm, from 341 nm, probably due to solvatochromism. In both samples containing THF, two shoulders with maxima at about 265 and 280 nm appear, which will be discussed below. No absorption bands above 430 nm with appreciable intensity are detected in all mixtures. The spectrum of the mixture with NM exhibits intense absorption below 400 nm due to the solvent cutoff, and no band can be identified. Instead, solutions of $FeCl_3$ in ACN (i.e., pure and mixed with CF) have a different UV-Vis profile compared to other solvents, with well-resolved bands at 360, 333, 268 and 240 nm. These bands are attributed to $[FeCl_4]^-$,[5-8] which is frequently observed in aqueous or organic mixtures of iron with excess chloride (absorption at 268 nm can have a contribution from CF).

The literature reports the formation of Fe(III) complexes with THF[9,10] and ACN,[10,11] for example $[FeCl_3(THF)]$ and $[FeCl_3(THF)_2]$ are reported for THF,[9,10] and cis-$[FeCl_2(CH_3CN)_4]^+[FeCl_4]^-$ is reported as crystals collected from the ACN solution,[10,11] but no consistent UV-Vis data is available. The UV-Vis spectra from Figure 4A show that only the mixtures with ACN present clear bands attributed to $[FeCl_4]^-$, although the other mixtures can have smaller contributions of these absorption bands that may be covered by other features. In aqueous media, $FeCl_3$ has been reported as able to produce aqueous complexes like $[FeCl_2(H_2O)_4]^+$ and species like $[FeCl_2]^+$ and $[FeCl_4]^-$ depending on chloride concentration.[6,8,10] In organic media, $FeCl_3$ can form monomers, dimers, solid particles and/or polymeric species,[12,13] and it also can form complexes like

$[FeCl_2]^+$, $[FeCl_4]^-$ or complexes with solvent molecules as ligands.[10] The amount of $[FeCl_4]^-$ formed is solvent-dependent, and ACN and NM can produce this complex with relatively high equilibrium constants.[14] All samples present high absorbance values below 250 nm due to solvent UV cut-offs, but the samples prepared in pure THF or pure ACN have a maximum at about 230-240 nm that can be resolved. There are two possible attributions for such bands: soluble monomeric $FeCl_3$[5,6] and complexes such as $[FeCl_2]^+$ and $[FeCl]^{2+}$.[6,8]

The sample made from chloroform and THF has higher absorption values between 250 and 280 nm than the mixtures with ACN. In pure THF or CF-THF, such bands can be attributed to soluble monomeric $FeCl_3$[5,6] or complexes having THF as a ligand. However, THF-based mixtures do not show a comparable absorbance of the other bands from 300 to 400 nm attributed to $[FeCl_4]^-$ characteristic of acetonitrile mixtures. This indicates the presence of neutral and/or cationic compounds in solutions with THF. For mixtures containing ACN, it is expected that cationic complexes are formed as reported,[10,11] because the starting solid has no net charge ($FeCl_3$) and an anion is detected. Our spectra confirm the presence of the anion $[FeCl_4]^-$ in pure ACN and CF-ACN. Interestingly, the mixture of CF-ACN presents bands of $[FeCl_4]^-$ with weaker absorbance than pure ACN, and a relatively small increase of the absorption at 341 nm ($FeCl_3$), due to the presence of CF in the mixture.

The mixture in CF-THF has solid particles as probed by DLS, and the soluble fraction is similar to that of CF mixture as probed by UV-Vis, however, it is not able to oxidise [3]Ph even at high concentrations. Since THF is a highly coordinating solvent, especially for hard Lewis acids[15,16] like Fe(III) complexes or free sites of solid $FeCl_3$ bearing non-coordinated Fe(III), our results indicate that THF-based mixtures are not able to promote [3]Ph oxidation because the surface of the dispersed nanoparticles are passivated by THF, decreasing the oxidation strength of the solid and producing a soluble fraction that is inactive as oxidiser. A similar behavior is expected by using the ethanol-stabilised CF,[17] but in this case [3]Ph was oxidised when the concentration of $FeCl_3$ overcomes a certain critical value, i.e., when there is no more "free" ethanol that can react with $FeCl_3$. It follows that solid $FeCl_3$ in THF or other highly coordinating solvents (e.g., ethanol) probably do not have free orbitals on the particle surface. A coordinated surface is non-active towards oxidation due to the absence of free Fe(III) orbitals, which could receive electrons.[12] Strong solvation can explain why even with solid nanoparticles, $FeCl_3$ in the mixture with THF was not able to promote oxidation of [3]Ph.

The ACN-based sample was chosen to probe the influence of the composition of soluble fractions on the reactivity of $FeCl_3$ since it was able to oxidise [3]Ph (Figure 1) and it presents clear bands in the UV-Vis-NIR. In **Figure S9B** the Raman spectra of $FeCl_3$ in solid state, pure solvents and CF-ACN mixture are shown. A Raman mode was identified at 283 cm^{-1}, in accordance with the

Raman spectrum of solid $FeCl_3$ at 298 K.[18] In solvents, the Raman profile of $FeCl_3$ changes completely. $FeCl_3$ in CF features Raman peaks at 262 and 367 cm^{-1}, which fully overlap with those of the spectrum of CF. $FeCl_3$ in ACN exhibits a Raman mode at 336 cm^{-1} (weak) and a broad band peaked at 383 cm^{-1}, with a shoulder close to 375 cm^{-1}. The latter is a vibration mode of ACN, whose Raman spectrum shows only one weak band at 376 cm^{-1}. $FeCl_3$ in the mixture of CF and ACN (1:1, volume) displays Raman modes at 262, 367 and 378 cm^{-1}.

Monomeric $FeCl_3$ in the gas phase has been assigned with a Raman mode at 370 cm^{-1}.[18] $FeCl_3$ in a pyramidal C_{3v} geometry, trapped in solid krypton, has Raman modes at 68.7, 113.8, 363 and 460.2 cm^{-1},[19] the peak at 363 cm^{-1} being the most intense. The dimer Fe_2Cl_6 has been assigned with Raman peaks at 314 and 422 cm^{-1} in gas phase,[18,20] the latter related to the frequency of the distorted bi-tetrahedral structure.[18] The same dimer trapped in solid krypton has two Raman modes at 315 and 426 cm^{-1},[19] the band at the higher frequency being the most intense. The anion $[FeCl_4]^-$ has Raman modes at about 120 and 332-334 cm^{-1},[8,18,21] the latter being attributed to the four-fold tetrahedral stretching.[18,21] The cation $[FeCl_2]^+$ has Raman active modes at 350 cm^{-1} in gas-phase and at ~390 cm^{-1} in melted mixtures of CsCl+$FeCl_3$ (with up to 75 % of $FeCl_3$, at 600 K).[22] The Raman modes of $FeCl_3$ experimentally observed in Raman spectra of **Fig. 4B** do not fit with any vibrations of $FeCl_3$ dimer. Thus, we can exclude its presence in the solutions studied here. Most bands detected in our Raman spectra are assigned to solvents' features, except for the band at 333 cm^{-1} observed for the mixture in pure ACN, which, based on the data in the literature, can be attributed to $[FeCl_4]^-$. The mode at 383 cm^{-1} for the same mixture can be attributed to cations like $[FeCl_2]^+$ and/or $[FeCl_2(CH_3CN)_4]^+$ (ACN vibration stiffening due to coordination). All the other samples have only Raman modes referent to the respective solvents. as discussed above. Raman data of **Fig. S9B** referent to the CF-ACN mixture does not present clear signs of anionic or cationic forms of $FeCl_3$, probably due to the lower concentration of these ions.

Fig. S10. (A) Pictures of homocoagulation experiments conducted with $FeCl_3$ (concentration of 0.75 g L^{-1}) in CF-ACN (1:1, volume) mixed with solutions of tetrabutylammonium tetrafluoroborate [(TBA)(TFB)] in different concentrations according to the internal labels (dissolved in the same liquid mixture). Bottom: pictures of the last three concentrations of $FeCl_3$ with [(TBA)(TFB)] irradiated with green laser on the right. (B) UV-Vis spectra of $FeCl_3$ (concentration of 0.05 g L^{-1}) in CF-ACN (1:1, volume) mixed with solutions of (TBA)(TFB) in different concentrations (10 mm cuvette). (C) Graphic of interaction energies as a function of distance calculated using DLVO theory for spherical particles and the values of mean radius (from DLS) and zeta potential (from homocoagulation experiment) for $FeCl_3$ in CF-ACN (1:1, volume). (D) UV-Vis-NIR spectra of [3]Ph mixed with $FeCl_3$ and [(TBA)(TFB)] 1×10^{-1} mol L^{-1} in CF-ACN (1:1, volume) (100 % is the original mixture and 1 % is diluted in the solvent mixture) (10 mm cuvette).

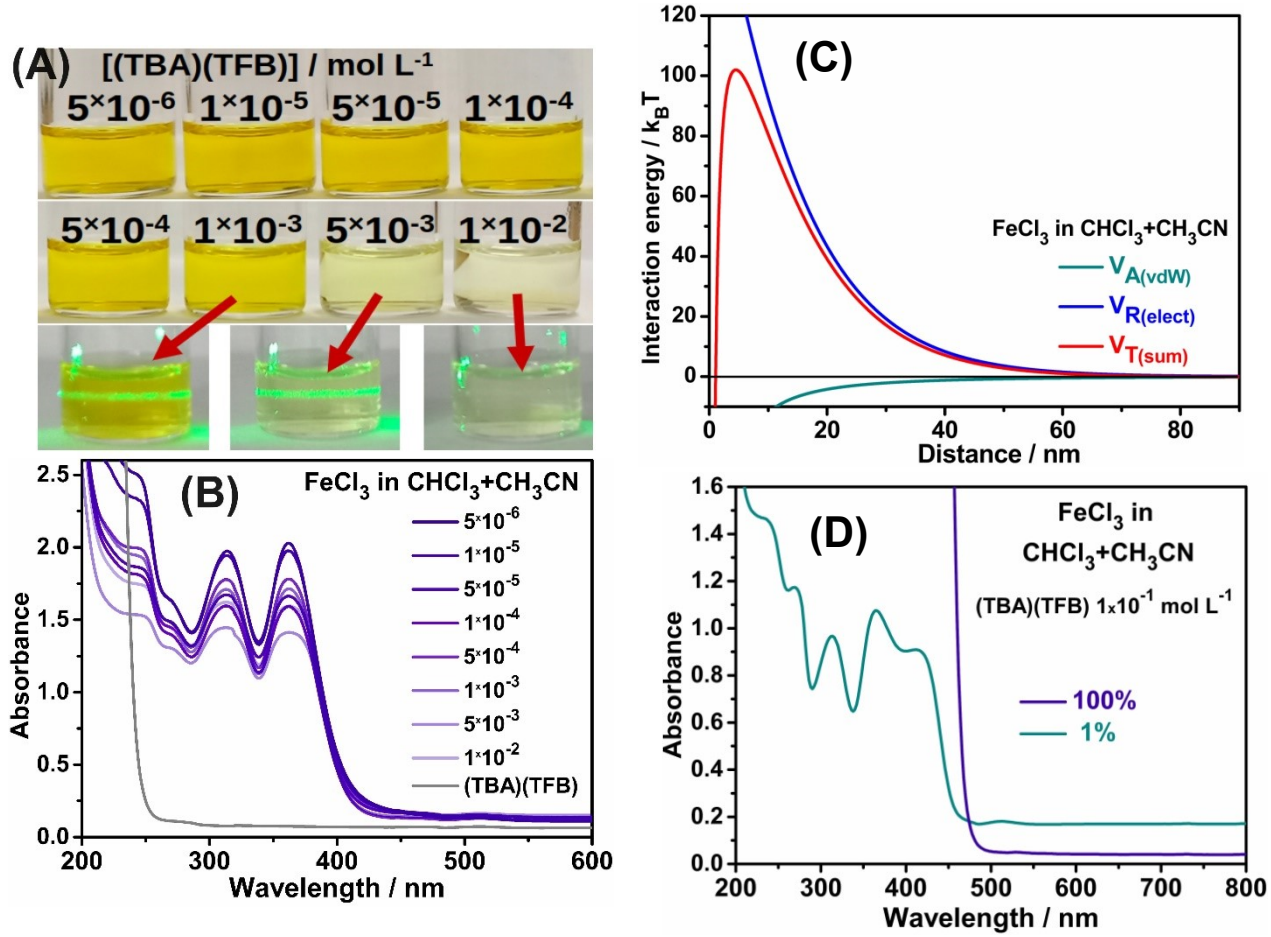

According to the reactivity hypothesis, THF (and ethanol) should passivate $FeCl_3$ particles, decreasing the oxidizing power. A surface passivated by solvent molecules indicates that the respective solid dispersion has colloidal stability mainly caused by solvation interactions.[23-25] However, particles of $FeCl_3$ in mixtures containing acetonitrile and nitromethane should behave as lyophobic colloids, having a scarce affinity for the solvent molecules. This type of colloid is stabilised

by electrostatic interactions.[23-25] A homocoagulation experiment was conducted with $FeCl_3$ in acetonitrile and chloroform mixture (1:1, volume) to evaluate the colloidal nature of this dispersion, chosen as a model system because it is oxidation-active for [3]Ph and presents clear UV-Vis bands. The result of homocoagulation is presented in **Fig. S10A**.

Solid particles of $FeCl_3$ coagulate in contact with relatively diluted electrolyte solutions, which is typical of lyophobic colloids.[23,24] This behavior indicates weak solvation, meaning that the solvent is not interacting strongly with the solid particles. So, the main source of colloidal stabilisation is electrostatic repulsion between dispersed nanoparticles of $FeCl_3$. This kind of stabilisation implies the presence of a non-zero zeta potential associated with the dispersed nanoparticles, therefore formal charges are separated at the solid-liquid interface, generating the zeta potential.[23] The vials containing $FeCl_3$ in contact with concentrated electrolyte do not present light scattering by the Tyndall effect, as presented in pictures from **Fig. S10A** (bottom), confirming the coagulation of colloidal particles and the precipitation of bulky solid material. Based on the colour change and absence of scattering, the critical coagulation concentration (CCC) was estimated as 5×10^{-3} mol L^{-1}, but it may be higher because this mixture still presents weak scattering.

The addition of electrolytes increases the mean diameter of the solid particles as shown by the DLS results in **Fig. S8**, which occurs until a threshold value of about 1 μm. Above this value, the colloidal forces (i.e., electrostatic repulsion) are not strong enough to maintain the particle dispersed. These DLS measurements indicate that the increase of ionic strength contributes to coagulation of the particles, as expected for a lyophobic colloid,[23,24] since it decreases the electrostatic repulsion by compressing the electrical double layer. However, in all mixtures, there are iron species that remain solubilised even at high electrolyte concentrations. This was evidenced by the UV-Vis spectra presented in **Fig. S10B**, which were acquired using the supernatants of diluted $FeCl_3$ mixtures in chloroform and acetonitrile mixed with the same organic electrolyte. The dilution of the $FeCl_3$ (15×) was necessary to avoid absorbance saturation, but the same trend is observed in relation to the mixtures presented in **Fig. S10A** in terms of coagulation and colour change. Therefore, the presence of soluble iron complexes is another indication of the colloidal nature of $FeCl_3$ in organic media because it is not a complete salting out upon adding electrolyte, but only the colloidal part of $FeCl_3$ is coagulating.

Considering the equation of CCC as a function of the physical properties of lyophobic colloids,[23,24] we can calculate the Stern potential (ψ_δ), which can be considered equal to the zeta potential (ζ) of the dispersed nanoparticle. Using the CCC value determined experimentally, the dielectric constant of the liquid medium (estimated as $\varepsilon = 21$), and the effective Hamaker constant of the particles (estimated as $A = 1\times10^{-19}$ J, relatively high and conservative value), we find a Stern potential of about |96| mV. Considering the absorbance value (A~2) from **Fig. S10B** and the value of

extinction molar coefficient (ε~1.1×10^4 M^{-1} cm^{-1}) for $[FeCl_4]^-$,[26] the anion concentration is about 1.82×10^{-4} mol L^{-1} for this mixture of acetonitrile and chloroform (1:1). This value was used to estimate the inverse Debye length (κ). The initial mixture had 0.05 g L^{-1} $FeCl_3$, which is equivalent to 3.08×10^{-4} mol L^{-1}, indicating that about 59 % (mol) of the initial salt produces $[FeCl_4]^-$ in this solvent mixture. We performed a calculation based on the Derjaguin-Landau-Verwey-Overbeek (DLVO) theory applied for spheres and considering the parameters described above, κ value equal to 8.57×10^7 m^{-1} (based on c = 0.182 mmol L^{-1}) and the mean radius of the nanoparticles (considered as 100 nm). This calculation is presented in a graphic in **Fig. S10C** and indicates an energy barrier close to 100×k_BT for the coagulation process, which is enough to maintain the solid nanoparticles dispersed for months (or years)[21,22,25] and corroborates the relatively high metastability of $FeCl_3$ particles over time.

The entire system is electrically neutral, so counter-ions are balancing the surface charge of the dispersed particles and forming the diffuse part of the electrical double layer around the particles. Although the Raman and UV-Vis bands of the complex $[FeCl_4]^-$ were detected (**Fig. S9**), signatures of the possible iron-based cations (counter-ions) were not confirmed, only suggested in UV-Vis and Raman spectra. Considering that all mixtures were prepared from neutral species, solid $FeCl_3$ and non-ionic solvents, we can postulate that the $FeCl_3$ nanoparticles in chloroform and acetonitrile mixtures are positively charged. Therefore, the anions $[FeCl_4]^-$ are the counter-ions of the colloidal particles in such mixtures, which indicates that the zeta potential estimated in the homocoagulation has a positive signal. This is a reasonable assumption, considering that the dispersed $FeCl_3$ nanoparticles have charges separated at the solid-liquid interface (non-zero zeta potential) and a possible negatively charged particle should not have much free iron(III) sites to allow the oxidation of organic molecules, because chloride anions would be in excess in this case. Unfortunately, $FeCl_3$ in organic media has a high oxidation potential making simple measurements of the zeta potential unfeasible.

Colloidal particles of other halides like AgBr or AgI dispersed in aqueous media have been studied for decades.[23,24,27-29] When no ionic surfactant is present, the surface charge and zeta potential of these colloidal dispersions have been attributed to (i) the formation of defects in the crystalline lattice and dissolution of anions or cations, or (ii) preferential adsorption of one type of lattice ion depending on the solution composition. Dissolution or adsorption is related to the different affinities of the ions with the liquid phase concerning the solid phase.[27] Silver halides usually present Frenkel defects[28] with displacing cations. Solid $FeCl_3$ most probably has Frenkel defects predominantly, with displaced anions due to the higher oxidation state and coordination number of cations.[30-31] The defect concentration is expected to be higher near the liquid-solid interface,[28,29,32] and chlorides from the surface can migrate to the solution and form the diffuse double layer, which

can be viewed as a non-stoichiometric defect forming a non-electrically-neutral-solid-((solid plus solution are electrically neutral). The 'excess' of $[FeCl_4]^-$ anions detected by UV-Vis and Raman measurements could arise from the complexation of Cl^- (from the unequal dissolution) with soluble $FeCl_3$. The formation of an electrical double layer and a non-zero zeta potential is important to stabilise these dispersions as discussed, but this is probably the source of such 'free sites' that are iron(III) with lower coordination numbers due to the 'release' of chlorides into the liquid phase, making the nanoparticles positively charged as we assumed. The mechanism of charge formation and the signal of the surface potential are currently under investigation.

Based on the CCC value (5×10^{-3} mol L^{-1}), the hypothesis that solid nanoparticles of $FeCl_3$ are necessary to promote oxidation was tested. A mixture of $FeCl_3$ (1.6 g L^{-1}) in chloroform and acetonitrile with [(TBA)(TFB)] 1×10^{-1} mol L^{-1} was prepared and mixed with [3]Ph (1.0 g L^{-1}). Just after adding the electrolyte, the dark yellow $FeCl_3$ mixtures turned light yellow due to the coagulation of solid particles. **Fig. S10D** shows the UV-Vis spectrum of that mixture, which does not have any absorption band in the visible region above 500 nm, indicating that the [3]Ph oxidation is not occurring. This mixture was diluted with the same solvent mixture (1:1, volume) to avoid saturation. The diluted system (1 %) exhibits bands in the UV region that indicate the presence of both soluble iron(III) compounds (below 360 nm) and the non-oxidised [3]Ph (band at 420 nm). This corroborates the hypothesis that the [3]Ph oxidation depends on the presence of solid $FeCl_3$ particles dispersed in organic solvents. Since all mixtures have soluble iron species, it is possible to conclude that most soluble compounds (e.g., $[FeCl_4]^-$) are inactive towards oxidation reactions as mentioned. Similarly, the presence of solid particles is also not directly correlated to [3]Ph oxidation, as highly coordinating solvents (e.g., THF) seem to block the surface of solid $FeCl_3$.

REFERENCES

[1] D. Wendinger, R. R. Tykwinski, *Acc. Chem. Res.* **2017**, *50*, 1468–1479.

[2] N. N. Greenwood, A. Earnshaw, *Chemistry of the Elements*, Butterworth-Heinemann, Woburn, USA, **2006**.

[3] J. Salinas-Luna, J. Mentado-Morales, *Phys. Scr.* **2024**, *99*, 015504.

[4] A. Ehlerding, I. Johansson, S. Wallin, H. Östmark, Int. J. Spectrosc., 2012, 1, 158715.

[5] P. E. Hoggard, M. Gruber, A. Vogler, *Inorganica Chim. Acta* **2003**, *346*, 137–142.

[6] W. Liu, B. Etschmann, J. Brugger, L. Spiccia, G. Foran, B. McInnes, *Chem. Geol.* **2006**, *231*, 326–349.

[7] I. E. Jacobs, Y. Lin, Y. Huang, X. Ren, D. Simatos, C. Chen, D. Tjhe, M. Statz, L. Lai, P. A. Finn, W. G. Neal, G. D'Avino, V. Lemaur, S. Fratini, D. Beljonne, J. Strzalka, C. B. Nielsen, S. Barlow, S. R. Marder, I. McCulloch, H. Sirringhaus, *Adv. Mater.* **2022**, *34*, 2102988.

[8] L. Cui, F. Cheng, J. Zhou, *Ind. Eng. Chem. Res.* **2015**, *54*, 7534–7542.

[9] F. A. Cotton, R. L. Luck, K. Son, *Acta Crystallogr. Sect. C Cryst. Struct. Commun.* **1990**, *46*, 1424–1426.

[10] S. A. Cotton, *J. Coord. Chem.* **2018**, *71*, 3415–3443.

[11] Y. Gao, J. Guery, C. Jacoboni, *Acta Crystallogr. Sect. C Cryst. Struct. Commun.* **1993**, *49*, 147–151.

[12] V. M. Niemi, P. Knuuttila, J.-E. Österholm, J. Korvola, *Polymer (Guildf).* **1992**, *33*, 1559–1562.

[13] A. Vertes, I. Nagy-Czako, K. Burger, *J. Phys. Chem.* **1978**, *82*, 1469–1473.

[14] T. B. Swanson, V. W. Laurie, *J. Phys. Chem.* **1965**, *69*, 244–250.

[15] J. E. Huheey, E. A. Keiter, R. L. Keiter, *Inorganic Chemistry: Principles of Structure and Reactivity*, HarperCollins College Publishers, New York, USA, **1993**.

[16] W. B. Jensen, *Chem. Rev.* **1978**, *78*, 1–22.

[17] T. Olinga, B. François, *Synth. Met.* **1995**, *69*, 297–298.

[18] G. N. Papatheodorou, G. A. Voyiatzis, *Chem. Phys. Lett.* **1999**, *303*, 151–156.

[19] A. Givan, A. Loewenschuss, *J. Raman Spectrosc.* **1977**, *6*, 84–88.

[20] P. J. Hodges, I. R. Beattie, J. M. Brown, *Phys. Chem. Chem. Phys.* **2006**, *8*, 2696.

[21] M. S. Sitze, E. R. Schreiter, E. V. Patterson, R. G. Freeman, *Inorg. Chem.* **2001**, *40*, 2298–2304.

[22] G. A. Voyiatzis, A. G. Kalampounias, G. N. Papatheodorou, *Phys. Chem. Chem. Phys.* **1999**, *1*, 4797–4803.

[23] D. J. Shaw, *Introduction to Colloid and Surface Chemistry*, Butterworth-Heinemann, Oxford, UK, **1992**.

[24] R. J. Hunter, *Foundations of Colloid Science*, Oxford University Press, New York, USA, **2001**.

[25] V. Agmo Hernández, *ChemTexts* **2023**, *9*, 10.

[26] Nomura, Y.; Inoue, D.; Moritomo, Y. Control of Fe^{3+} Coordination by Excess Cl^- in Alcohol Solutions. *RSC Adv.* **2022**, *12* (28), 17932–17936.

[27] Kakiuchi, T.; Samec, Z. An Electrochemical Viewpoint on the Solubility of Silver Halides in Water. *J. Solid State Electrochem.* **2020**, *24* (11–12), 3185–3189.

[28] Grimley, T. B. The Contact between a Solid and an Electrolyte. *Proc. R. Soc. London. Ser. A. Math. Phys. Sci.* **1950**, *201* (1064), 40–61.

[29] Ottewill, R..; Woodbridge, R. Studies on the Electrokinetic Behavior of Monodisperse Silver Halide Sols. *J. Colloid Sci.* **1964**, *19* (7), 606–620. DOI: 10.1016/0095-8522(64)90084-4.

[30] Greenwood, N. N. *Ionic Crystals, Lattice Defects and Nonstoichiometry*; Butterworth & Co: London, UK, **1968**.

[31] West, A. R. *Solid State Chemistry and Its Applications*, 2nd ed.; John Wiley & Sons: Chichester, United Kingdom, **2014**.

[32] Grimley, T. B.; Mott, N. F. I. General and Theoretical. The Contact between a Solid and a Liquid Electrolyte. *Discuss. Faraday Soc.* **1947**, *1*, 3.